Mathematical Model of Dengue Virus with Primary and Secondary Infection

Rattiya Sungchasit[1] and Puntani Pongsumpun[2*]

[1]Department of Mathematics, Faculty of Science and Technology,
Phuket Rajabhat University, Phuket, Thailand
[2]Department of Mathematics, Faculty of Science,
King Mongkut's Institute of Technology Ladkrabang, Bangkok, Thailand

Received: 22 January 2019, Revised: 7 May 2019, Accepted: 7 May 2019

Abstract

In this study, we analyzed an SEIR model for human and SEI model for mosquitoes. We considered the development of dengue infection from dengue fever (DF) to dengue hemorrhagic fever (DHF). The stability of the endemic equilibrium and the disease-free equilibrium states are incurred by Routh-Hurwitz criteria. Numerical simulations for the model are used to solve a system of differential equations. It showed that the local stability for disease free states and endemic states are depend on the basic reproductive rate of the disease. The results of this study is recommended as an effective control measure for reducing the transmission of dengue disease.

Keywords: dengue fever, SEIR model, SEI model
DOI……

1. Introduction

Dengue is a violent infectious disease that occurs in tropical and sub-tropical regions, being one of the average harsh arthropod borne viral disease in group of human death and morbidity [1-5]. Dengue virus occurs due to an infection of the *Flaviviridae* family. Four serotypes of the dengue virus, namely DENV-1, -2, -3 and -4 have been identified as the main causes of the infection. An infection with any types of these viruses may be asymptomatic or causing temperature sickness known as dengue fever (DF). Such epidemic occurs due to atmosphere change and limited understanding of the degenerate native of the dengue disease. The World Health Organization (WHO) has reported approximately 50 -100 million cases globally, including 50,000 infected with dengue hemorrhagic fever (DHF) or dengue shock syndrome(DSS) annually [1, 6-9, 10-12]. The main prevalence of this epidemic disease is in Central American, Southeast Asia and South Asia [11-16].

*Corresponding author: Tel.: 662-329-8000 Ext. 6196 Fax: 662-329-8412
E-mail: kppuntan@kmitl.ac.th

Since preliminary symptoms of the DFF/DSS and DF are similar, a relatively short period of infection further complicates the diagnosis of the disease, as well as of the possible person having the capacity of spreading severe transpriation. DHF represents a separate pathophysiological procedure or is only the opposite end of a continuation of identical diseases. DF follows a change from the normal but rather a danger self-inclined course. DHF may show as a relatively mild infection at first, but can quickly develop into life-menacing disease as fever reduces. DHF can mainly be distinguished from the usual dengue fever due to its three predictable classification phrases [4,13].

WHO classifies the type of DF based on the severity of illness. Classic dengue fever "break bone fever" is identified by beginning of a high fever. The symptom appears 3 to 14 days after the biting of infected mosquitoes. The characteristics of DF are myalgia, headache, rash and arthralgias. As the fever begins to subside 3 to 7 days after first appearance of the symptom, the patient may have complete resolution of symptoms, or go on to develop DHF. It assorts dengue virus as with or without forewarning covenant (aching belly, retaining, severe vomiting, mucosal hemorrhage, nausea and sleepiness, high hematocrit with low thrombocytes) and violent dengue (violent plasma puncture, violent hemorrhage, or stalk naught) [9, 13-18]. Cases of DHF are defined by four characteristics: recent history of any hemorrhagic manifestation fever, thrombocytopenia, and evidence of increased vascular permeability. Cases of dengue shock syndrome meet the four criteria for DHF, but also show signs of circulatory failure, rapid, narrow pulse pressure, such as a weak pulse or hypotension. The risk of progression to DHF or DSS is increased in secondary infections when the individual has been infected previously by a different virus serotype [16-21].

Many researches have applied mathematical model to describe the transmission of the dengue fever. The work of Sungchasit and Pongsumpun [8] used SEIR model to describe the transmission of dengue disease between human and mosquito in each season. An SIR model was used to study the transmission of dengue infection with two types of mosquitoes such as *Aedes aegypti* and *Aedes albopictus* mosquitoes [22]. Khalid *et al*. [17] studied about the clinical course and IgG/IgM ratio is used to separate the different between primary and secondary infections. Esteva and Vargas [7] used SIR model for describing the transmission of dengue fever in a constant human population and variable vector population. Syafruddin and Noorani [14] studied the system of differential equations for the dynamics of SEIR model for DF. For more detailed prediction of the epidemic, it is necessary to examine the higher order moments, namely the variance of the number of infected. So, the predictability of mean-field models depends on the variations around the mean [22-25] In this work, we focus on the mathematical model of dengue disease with the development of dengue infection from DF to DHF.

2. Mathematical model

We use mathematical model to formulate the dynamical equations between human and mosquitoes populations. The development of dengue infection from DF to DHF is considered. We separate the human population into 4 groups, namely the Susceptible group (S), Exposed group (E), Infectious group (I) and Recovered group (R). The infectious group is further subdivided into two subclasses, those infected with DF, and those whose disease has morphed into DHF. The mosquitoes populations are subdivided into 3 groups, namely Susceptible group (S), Exposed group (E) and Infectious group (I) because the mosquitoes do not recover from infection. The basis of evidence is that all human population and mosquito population possess fixed rate sizes [6-8, 15, 17]. The characteristics of dengue fever transmission can be described through a state transition diagram as shown in Figures 1-2 [7, 17, 21]. The variables and parameters for model is explained in Table 1.

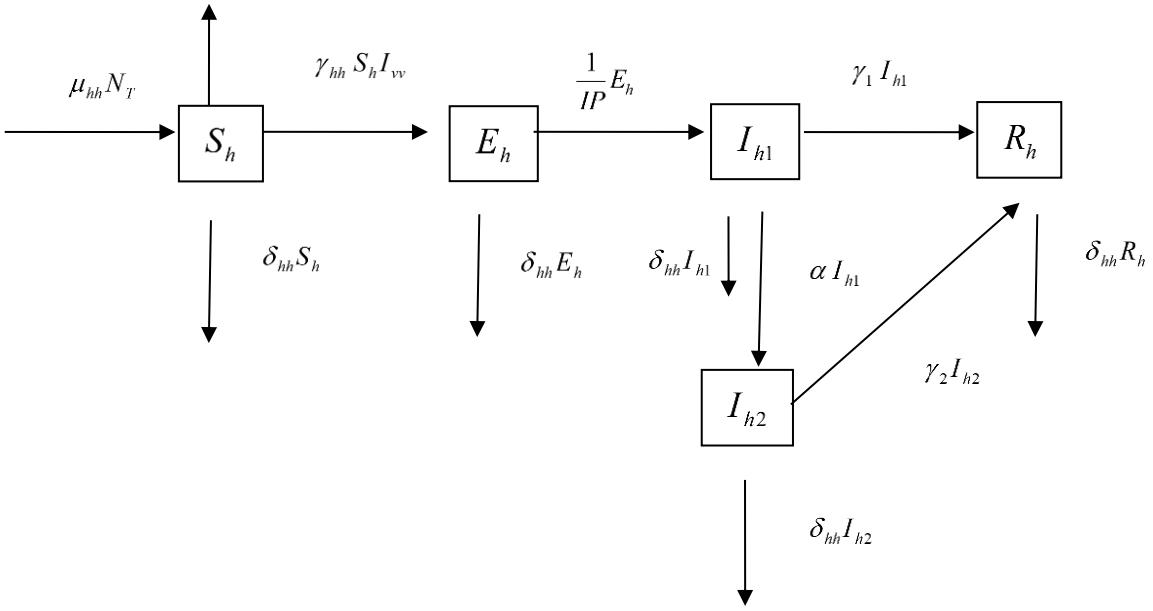

Figure 1. The state transition diagram for the human population

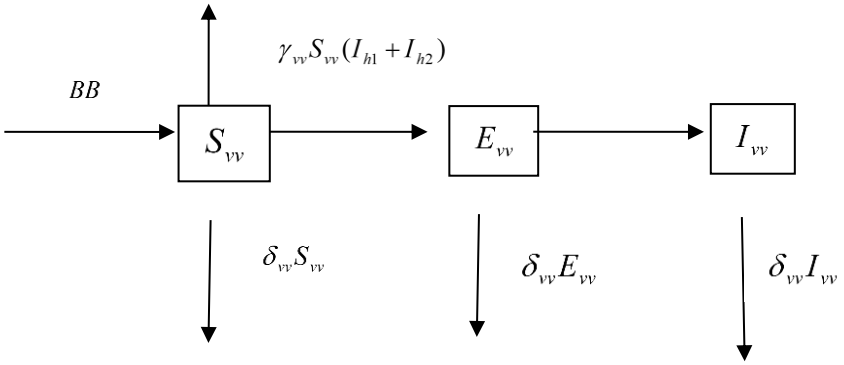

Figure 2. The state transition diagram for the mosquito population

Table 1. The variables and parameters in model

Variables/ parameters	Description
S_h	The number of susceptible human population
E_h	The number of exposed human population (infected but not yet transmit the dengue virus)
I_{h1}	The number of DF patients
I_{h2}	The number of DHF patients
R_h	The number of recovery human population
S_{vv}	The number of susceptible mosquito population
E_{vv}	The number of exposed mosquito population (infected but not yet transmit the dengue virus)
I_{vv}	The number of infectious mosquito population
μ_{hh}	The birth rate of human population
δ_{hh}	The death rate of human population
N_T	The total human population
γ_{hh}	The transmission probability of dengue virus from mosquito to human
$\frac{1}{IP}$	Incubation rate of dengue virus in human population
γ_1	The recovery rate of DF cases
γ_2	The recovery rate of DHF cases
γ_{vv}	The transmission probability of dengue disease from human to mosquitoes
α	The rates of change from DF cases to DHF cases
BB	The recruitment rate of mosquitoes
N_v	The total mosquitoes
δ_{vv}	The death rate of mosquitoes
$\frac{1}{EP}$	The incubation rate of dengue virus in mosquito population

From the state transition diagram of Figure 1, the following system of differential equations is written for the human population.

$$\frac{dS_h}{dt} = \mu_{hh} N_T - \gamma_{hh} S_h I_w - \delta_{hh} S_h \quad (1)$$

$$\frac{dE_h}{dt} = \gamma_{hh} S_h I_w - \delta_{hh} E_h - \frac{1}{IP} E_h \quad (2)$$

$$\frac{dI_{h1}}{dt} = \frac{1}{IP} E_h - \delta_{hh} I_{h1} - \gamma_1 I_{h1} - \alpha I_{h1} \quad (3)$$

$$\frac{dI_{h2}}{dt} = \alpha I_{h1} - \delta_{hh} I_{h2} - \gamma_2 I_{h2} \quad (4)$$

$$\frac{dR_h}{dt} = \gamma_1 I_{h1} + \gamma_2 I_{h2} - \delta_{hh} R_h \quad (5)$$

Similarly, the state transition diagram of Fig. 2 admits the following system of differential equations for the mosquito population.

$$\frac{dS_w}{dt} = BB - \gamma_w S_w (I_{h1} + I_{h2}) - \delta_w S_w \quad (6)$$

$$\frac{dE_w}{dt} = \gamma_w S_w (I_{h1} + I_{h2}) - \delta_w E_w - \frac{1}{EP} E_w \quad (7)$$

$$\frac{dI_w}{dt} = \frac{1}{EP} E_w - \delta_w I_w \quad (8)$$

Therefore, the rate of changes for total human and mosquito populations is equal to zero. From setting $\frac{dN_T}{dt} = 0$ and $\frac{dN_w}{dt} = 0$, we can have $\mu_{hh} = \delta_{hh}$. Birth rates and death rates are equivalent for human population. For mosquito population, we have $\mu_w = BB$

We introduce the normalized variables

$S'_h = \frac{S_h}{N_T}, E'_h = \frac{E_h}{N_T}, I'_{h1} = \frac{I_{h1}}{N_T}, I'_{h2} = \frac{I_{h2}}{N_T}, R'_h = \frac{R_h}{N_T}$ and

$S'_w = \frac{S_w}{N_w}, E'_w = \frac{E_w}{N_w}, I'_w = \frac{I_w}{N_w}$, then the reduced equations become

$$\frac{dS'_h}{dt} = \mu_{hh} - \gamma_{hh} S'_h I'_w N_w - \delta_{hh} S'_h \quad (9)$$

$$\frac{dE'_h}{dt} = \gamma_{hh} S'_h I'_{hv} N_w - \delta_{hh} E'_h - \frac{1}{IP} E'_h \quad (10)$$

$$\frac{dI'_{h1}}{dt} = \frac{1}{IP} E'_h - \delta_{hh} I'_{h1} - \gamma_1 I'_{h1} - \alpha I'_{h1} \quad (11)$$

$$\frac{dI'_{h2}}{dt} = \alpha I'_{h1} - \delta_{hh} I'_{h2} - \gamma_2 I'_{h2} \quad (12)$$

$$\frac{dE'_{vv}}{dt} = \gamma_{vv}(1-E'_{vv}-I'_{vv})(I'_{h1}N_T + I'_{h2}N_T) - \delta_{vv}E'_{vv} - \frac{1}{EP}E'_{vv} \quad (13)$$

$$\frac{dI'_{vv}}{dt} = \frac{1}{EP}E'_{vv} - \delta_{vv}I'_{vv} \quad (14)$$

with the conditions $S'_h + E'_h + I'_{h1} + I'_{h2} + R'_h = 1$ and $S'_{vv} + E'_{vv} + I'_{vv} = 1$

3. Analysis of Mathematical Model

We analyze the formulated model and described the variant region and the positive of solutions. The feasible solution set of systems enter the region with the initial conditions is as follows:

$$\Omega = \{(S_h, E_h, I_{h1}, I_{h2}, E_{vv}, I_{vv}) : 0 \le S_h + E_h + I_{h1} + I_{h2} \le 1; E_{vv} + I_{vv} \le 1\}.$$

We will just define the conditions for local stability though an analysis of the boundaries of the areas where the equilibrium points are in Ω [22].

3.1 Equilibrium points

The equilibrium points are incurred by setting the righthand side of equations (9)-(14) equal to zero. We obtained the equilibrium points as follows: [7, 22]

Disease free equilibrium point:

$$P_0 = (\frac{\mu_{hh}}{\delta_{hh}}, 0, 0, 0, 0, 0)$$

Endemic equilibrium point:

$$P_1 = (S_h^*, E_h^*, I_{h1}^*, I_{h2}^*, E_{vv}^*, I_{vv}^*)$$

where

$$S_h^* = \frac{\mu_{hh}}{\delta_{hh} + I_{vv}^* N_{vv} \gamma_{hh}},$$

$$E_h^* = \frac{IP\, I_{vv}^* N_{vv} \gamma_{hh} \mu_{hh}}{(1+\delta_{hh}\, IP)(\delta_{hh} + I_{vv}^* N_{vv} \gamma_{hh})},$$

$$I_{h1}^* = \frac{I_{vv}^* N_{vv} \gamma_{hh} \mu_{hh}}{(1+\delta_{hh}\, IP)(\delta_{hh} + \alpha + \gamma_1)(\delta_{hh} + I_{vv}^* N_{vv} \gamma_{hh})},$$

$$I_{h2}^* = \frac{I_{vv}^* N_{vv} \gamma_{hh} \mu_{hh} \alpha}{(1+\delta_{hh}\, IP)(\delta_{hh} + \alpha + \gamma_1)(\delta_{hh} + I_{vv}^* N_{vv} \gamma_{hh})(\delta_{hh} + \gamma_2)}, \quad E_{vv}^* = \frac{EP\,(I_{h1}^* + I_{h2}^*)(-1 + I_{vv}^*) N_T \gamma_{vv}}{1 + EP\,((I_{h1}^* + I_{h2}^*) N_T \gamma_{vv} + \mu_{vv}}},$$

$$I_{vv}^* = \frac{(N_T N_{vv}(\delta_{hh} + \alpha + \gamma_2)\gamma_{hh}\gamma_{vv}\mu_{hh} - \delta_{hh}(1+\delta_{hh}IP)(\delta_{hh}+\alpha+\gamma_1)(\delta_{hh}+\gamma_2)\mu_{vv} - \delta_{hh}EP(1+\delta_{hh}IP)(\delta_{hh}+\alpha+\gamma_1)(\delta_{hh}+\gamma_2)\mu_{vv}^2)}{N_{vv}\gamma_{hh}(1+EP\mu_{vv})(N_T(\delta_{hh}+\alpha+\gamma_2)\gamma_{vv}\mu_{hh} + (1+\delta_{hh}IP)(\delta_{hh}+\alpha+\gamma_1)(\delta_{hh}+\gamma_2)\mu_{vv}}$$

3.2 Stability analysis

Theorem 3.2.1 Disease free equilibrium point of the method is locally asymptotically stable if $R_0 < 1$ and unstable if $R_0 > 1$.

Proof: We consider the equations

$$S_h = \mu_{hh} - \gamma_{hh} S_h' I_{vv}' N_{vv} - \delta_{hh} S_h' \tag{15}$$

$$E_h = \gamma_{hh} S_h' I_{vv}' N_{vv} - \delta_{hh} E_h' - \frac{1}{IP} E_h' \tag{16}$$

$$I_{h1} = \frac{1}{IP} E_h' - \delta_{hh} I_{h1}' - \gamma_1 I_{h1}' - \alpha I_{h1}' \tag{17}$$

$$I_{h2} = \alpha I_{h1}' - \delta_{hh} I_{h2}' - \gamma_2 I_{h2}' \tag{18}$$

$$E_{vv} = \gamma_{vv}(1 - E_{vv}' - I_{vv}')(I_{h1}' N_T + I_{h2}' N_T) - \delta_{vv} E_{vv}' - \frac{1}{EP} E_{vv}' \tag{19}$$

$$I_{vv} = \frac{1}{EP} E_{vv}' - \delta_{vv} I_{vv}' \tag{20}$$

The eigenvalues are computed from the solutions of the characteristic equation $|S - \lambda I| = 0$, where S is the Jacobian matrix at the equilibrium point and I is the identity matrix of dimension 6x6. If all the eigenvalues have negative real parts, then the equilibrium point is locally stable [7].

The Jacobian matrix evaluated at $P_0 = (\frac{\mu_{hh}}{\delta_{hh}}, 0, 0, 0, 0, 0)$ is given as

$$S_0 = \begin{pmatrix} -(\delta_{hh}) & 0 & 0 & 0 & 0 & -\gamma_{hh}(\frac{\mu_{hh}}{\delta_{hh}})N_{vv} \\ 0 & -(\delta_{hh} + \frac{1}{IP}) & 0 & 0 & 0 & \gamma_{hh}(\frac{\mu_{hh}}{\delta_{hh}})N_{vv} \\ 0 & \frac{1}{IP} & -(\delta_{hh} + \gamma_1) & \alpha & 0 & 0 \\ 0 & 0 & 0 & -(\delta_{hh} + \gamma_2) & 0 & 0 \\ 0 & 0 & \gamma_{vv}(N_T) & \gamma_{vv}(N_T) & -\mu_{vv} - ((1/EP))) & -((0) + (0))\, N_T\, \gamma_{vv} \\ 0 & 0 & 0 & 0 & \frac{1}{EP} & -\mu_{vv} \end{pmatrix}.$$

The characteristic equation is given as

$$\lambda^6 + A_1\lambda^5 + A_2\lambda^4 + A_3\lambda^3 + A_4\lambda^2 + A_5\lambda^1 + A_6 = 0,$$

where

$$A_1 = 4\delta_{hh} + \frac{1}{EP} + \frac{1}{IP} + 2\left(\gamma_1 + \gamma_2 + 2\mu_w\right) \tag{21}$$

$$A_2 = \frac{1}{EP\ IP}(1 + 6{\delta_{hh}}^2\ EP\ IP + IP(\gamma_1 + \gamma_2 + \mu_w) + EP(\gamma_1 + \gamma_2 + IP\gamma_1\gamma_2 + 2(1 + IP(\gamma_1 + \gamma_2))\mu_w + IP\ {\mu_w}^2) + \delta_{hh}(4IP + EP(3 + 3IP(\gamma_1 + \gamma_2) + 8\ IP\mu_w))) \tag{22}$$

$$A_3 = \frac{1}{EP\ IP}(4{\delta_{hh}}^3 EP\ IP + \gamma_1 + \gamma_2 + (EP + IP)\gamma_1\gamma_2 + \mu_w + (IP(\gamma_1 + \gamma_2) + 2EP(\gamma_1 + \gamma_2 + IP\gamma_1\gamma_2))\mu_w + EP(1 + IP(\gamma_1 + \gamma_2))\mu_w{}^2 + \delta_{hh}(3 + 3IP(\gamma_1 + \gamma_2) + 4\ IP\mu_w + 2EP\ (\gamma_1 + \gamma_2 + IP\gamma_1\gamma_2 + 3(1 + IP(\gamma_1 + \gamma_2))\mu_w + 2IP\mu_w{}^2)) + 3{\delta_{hh}}^2(2IP + EP(1 + IP(\gamma_1 + \gamma_2 + 4\mu_w)))) \tag{23}$$

$$A_4 = \frac{1}{EP\ IP}(-N_T N_w \gamma_{hh}\gamma_w\mu_{hh} + \delta_{hh}({\delta_{hh}}^4 EP\ IP + \gamma_1\gamma_2 + (\gamma_1 + \gamma_2 + (2\,EP + IP)\gamma_1\gamma_2)\mu_w + EP(\gamma_1 + \gamma_2 + IP\gamma_1\gamma_2)\ \mu_w{}^2 + \delta_{hh}(2\gamma_1 + 2\gamma_2 + EP\gamma_1\gamma_2 + 2IP\,\gamma_1\gamma_2 + (3 + 3IP(\gamma_1 + \gamma_2) + 4EP(\gamma_1 + \gamma_2 + IP\gamma_1\gamma_2))\ \mu_w + 3EP(1 + IP(\gamma_1 + \gamma_2))\mu_w{}^2) + {\delta_{hh}}^2(3 + 3IP(\gamma_1 + \gamma_2 + 2\mu_w) EP(\gamma_1 + \gamma_2 + IP\gamma_1\gamma_2 + 6(1 + IP(\gamma_1 + \gamma_2))\mu_v + 6IP\mu_w{}^2)) + {\delta_{hh}}^3(4IP + EP(1 + IP(\gamma_1 + \gamma_2 + 8\mu_w))))) \tag{24}$$

$$A_5 = \frac{1}{EP\ IP}(-N_T N_w \gamma_{hh}\gamma_w\mu_{hh} + \delta_{hh}({\delta_{hh}}^4 EP\ IP + \gamma_1\gamma_2 + (\gamma_1 + \gamma_2 + (2\,EP + IP)\gamma_1\gamma_2)\mu_w + EP(\gamma_1 + \gamma_2 + IP\gamma_1\gamma_2)\ \mu_w{}^2 + \delta_{hh}(2\gamma_1 + 2\gamma_2 + EP\gamma_1\gamma_2 + 2IP\gamma_1\gamma_2 + (3 + 3IP(\gamma_1 + \gamma_2) + 4EP(\gamma_1 + \gamma_2 + IP\gamma_1\gamma_2))\ \mu_w + 3EP(1 + IP(\gamma_1 + \gamma_2))\mu_w{}^2) + {\delta_{hh}}^2(3 + 3IP(\gamma_1 + \gamma_2 + 2\mu_w) EP(\gamma_1 + \gamma_2 + IP\gamma_1\gamma_2 + 6(1 + IP(\gamma_1 + \gamma_2))\mu_w + 6IP\mu_w{}^2)) + {\delta_{hh}}^3(4IP + EP(1 + IP(\gamma_1 + \gamma_2 + 8\mu_w))))) \tag{25}$$

$$A_6 = \frac{(\delta_{hh} + \gamma_2)(-N_T N_w \gamma_{hh}\gamma_w\mu_{hh} + \delta_{hh}(1 + \delta_{hh} IP)(\delta_{hh} + \gamma_1)\mu_w(1 + EP\mu_w))}{EP\ IP} \tag{26}$$

All six eigenvalues possess negative real parts, if they satisfy the Routh-Hurwitz criteria. Hence the equilibrium point is locally asymptotically stable if the following conditions are satisfied [7-9, 11, 13, 19].

$$A_1A_2 > A_3 \tag{27}$$

$$A_1A_2A_3 > A_3^2 + A_1^2A_4 \tag{28}$$

$$A_2A_3\ A_5 + A_1A_4(A_2A_3 + A_5)\ > A_4(A_3^2 + A_1^2A_4) + A_1A_2^2A_5 \tag{29}$$

$$A_2A_3\ A_5^2 + A_1A_4A_5\ (A_2A_3 + 2A_5)\ +\ A_3^3A_6 + A_1^2(A_3A_4 + 2A_2A_5)\ A_6 > A_5(A_4(A_3^2 + A_1^2A_4) + A_1A_2^2A_5 + A_5^2) + A_1A_3(A_2A_3 + 3A_5)A_6 + A_1^3A_6^2 \tag{30}$$

The conditions of Equations (27)-(30) are investigated numerically. Figure 3 plots the results of this investigation. It is evident that if $R_0 < 1$, the Routh-Hurwitz criteria is satisfied.

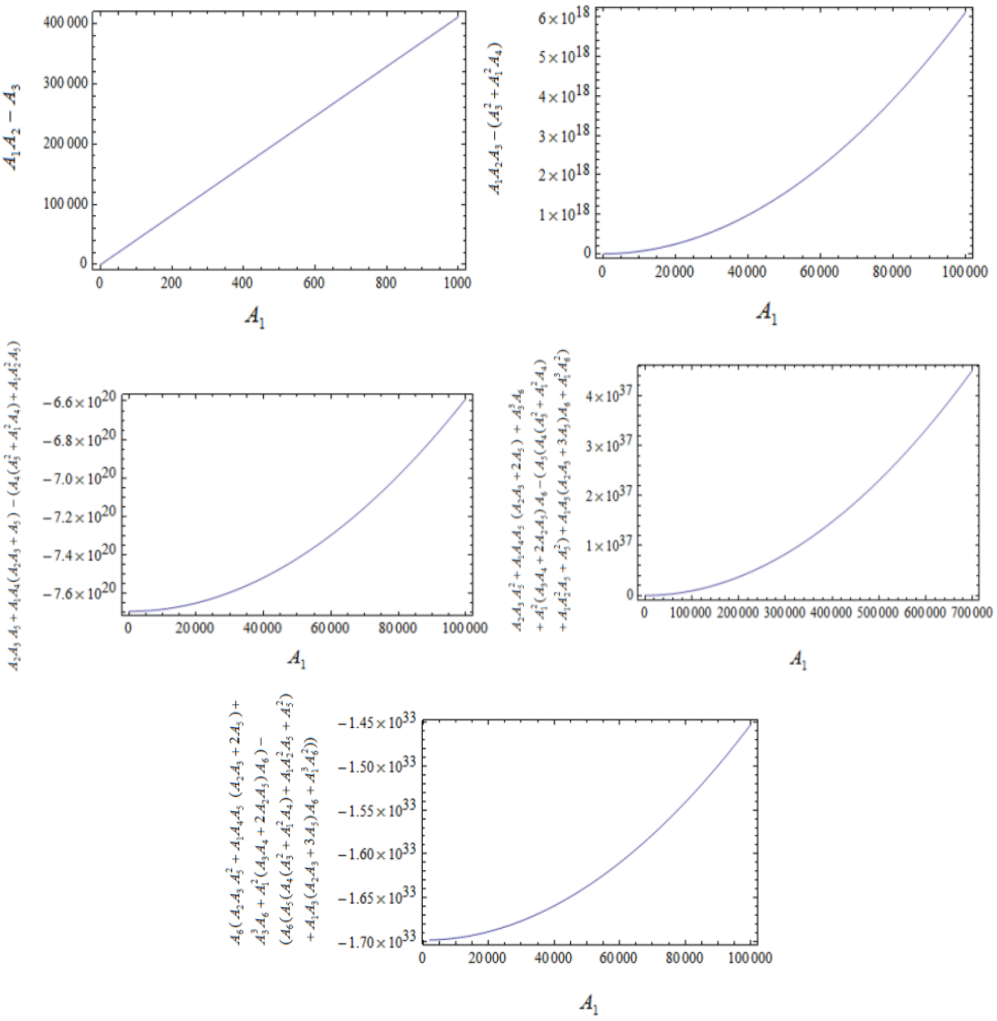

Figure 3. The parameter spaces of disease-free equilibrium point that influences the Routh-Hurwitz criteria with the value of parameters, respectively with $\gamma_1 = 0.178$, $\delta_{hh} = 1/(365*74)$, $\gamma_{hh} = 0.5$, $\gamma_w = 0.8$, $\gamma_2 = 0.4$, $EP = 0.87$, $\alpha = 0.001$, $IP = 0.09$, $N_T = 100,000$, $N_w = 5{,}000$

Each subfigures of Figure 3 shows the values for each condition of Equations (27)- (30) where the parameter A_1 is changed and the other parameters are kept fixed. It is evident that the Routh-Hurwitz situations are satisfied for the case of $R_0 < 1$.

Theorem 3.2.2 If $R_0 > 1$, the endemic equilibrium stable P_1 is locally asymptotically stable.

Proof: The Jacobian matrix is evaluated on the endemic equilibrium point $P_1 = (S_h^*, E_h^*, I_{h1}^*, I_{h2}^*, E_{vv}^*, I_{vv}^*)$ as given by

$$S_1 = \begin{pmatrix} -(\gamma_{hh} I_w^* N_w + \delta_{hh}) & 0 & 0 & 0 & 0 & -\gamma_{hh} S_h^* N_w \\ \gamma_{hh} I_w^* N_w & -(\delta_{hh} + \frac{1}{IP}) & 0 & 0 & 0 & \gamma_{hh} S_h^* N_w \\ 0 & \frac{1}{IP} & -(\delta_{hh} + \gamma_1) & \alpha & 0 & 0 \\ 0 & 0 & 0 & -(\delta_{hh} + \gamma_2) & 0 & 0 \\ 0 & 0 & \gamma_w(1 - E_w' - I_w')(N_T) & \gamma_w(1 - E_w' - I_w')(N_T) & (-(I_{h1}^* + I_{h2}^*) N_t \gamma_w - \mu_w - ((1/EP))) & -(I_{h1}^* + I_{h2}^*) N_T \gamma_w \\ 0 & 0 & 0 & 0 & \frac{1}{EP} & -\mu_w \end{pmatrix}$$

The six eigenvalues are again found from solving the characteristic equation.

$$\lambda^6 + D_1\lambda^5 + D_2\lambda^4 + D_3\lambda^3 + D_4\lambda^2 + D_5\lambda^1 + D_6 = 0 \tag{31}$$

The solution of Equation (31) will yield negative real parts if the Routh-Hurwitz criteria is satisfied. That is, if the conditions of Equations (27)-(30) are satisfied, with $A_i = D_i$, i = 1, 2, 3, 4, 5 and 6.

To simplify the computations, numerical analysis into conditions laid out in Equations (27)-(30) was conducted in similar fashion to the disease-free case. Figure 4 plots the results of the investigations. It is seen that the Routh-Hurwitz criteria will be satisfied for $R_0 > 1$.

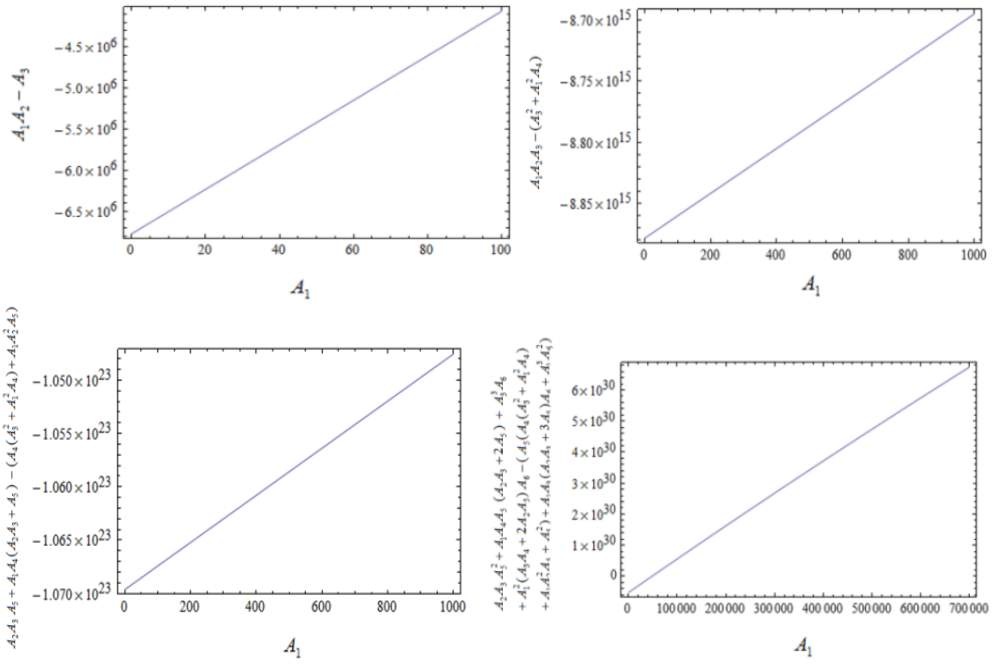

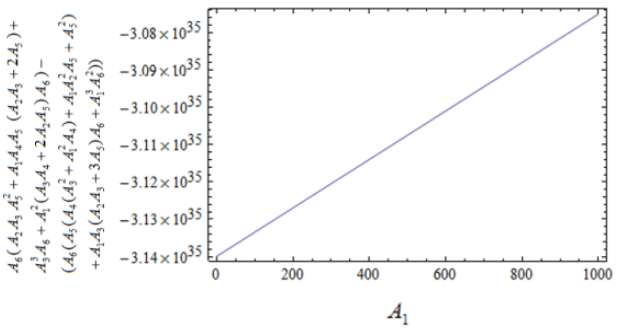

Figure 4. The parameter spaces in support of endemic equilibrium point which convinces the Routh - Hurwitz criteria with the values of parameters: respectively with $\gamma_1 = 0.178$, $\delta_{hh} = 1/(365*74)$, $\gamma_{hh} = 0.5$, $\gamma_w = 0.8$, $\gamma_2 = 0.4$, $EP = 0.87$, $\alpha = 0.006$, $IP = 0.09$, $N_T = 600{,}000$, $N_w = 30{,}000$.

From Figure 4, the Routh-Hurwitz conditions are satisfied in the case of $R_0 > 1$. Each figure shows the values for each condition when there is the variation of the parameter A_1. We can see that the Routh Hurwitz criteria of Equations (27)-(30) are again satisfied.

3.3 Numerical Simulation

From practical point of view, numerical results are very important for any analysis. In our study, we suggested the mathematical model in support of dengue disease considering the development of dengue disease from DF to DHF. We also performed the numerical solutions by using set of parameter values. We considered the dynamics of our model for our model for both disease-free and endemic states. The parameter values used in this study are given in Table 2. The numerical results are shown in Figures 5-7 [6, 8, 11, 13, 15, 17].

Table 2. Parameters used in simulations for secondary dengue fever.

Parameter	Biological meaning	Values
μ_{hh}	The birth rate of human population	$\frac{1}{(365*74)}$ per day
δ_{hh}	The death rate of human population	$\frac{1}{(365*74)}$ per day
N_T	The total human population	300,000 per day
γ_{hh}	The transmission probability of dengue virus from mosquito to human	0.01 – 0.009
$\frac{1}{IP}$	The incubation rate of dengue virus in human population	0.01 – 0.000009 per day
γ_1	The recovery rate of DF cases	0.1 – 0.09 per day

Table 2. (cont.)

γ_2	The recovery rate of DHF cases	0.1 – 0.9 per day
γ_{vv}	The transmission probability of dengue disease from human to mosquito	0.1 – 0.99
BB	The recruitment rate of mosquitoes	0.1 – 0.9 per day
N_{vv}	The total mosquitoes	200 - 100,000 per day
δ_{vv}	The death rate of mosquitoes	0.1 – 0.0007 per day
$\frac{1}{EP}$	The incubation rate of dengue virus in mosquito population	0.01 – 0.0087 per day
α	The rates of change from DF cases to DHF cases	0.1 - 0.9 per day

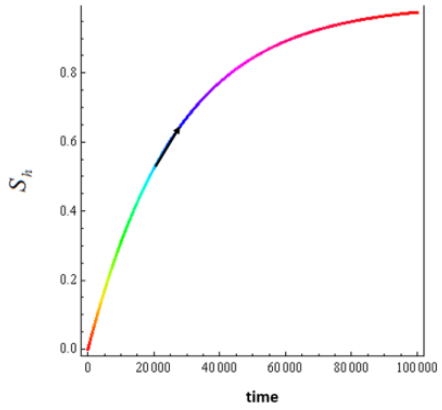

(aa)

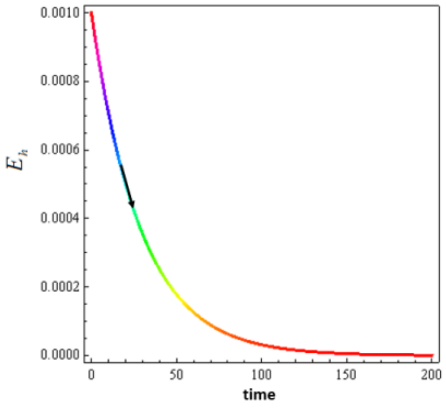

(ab)

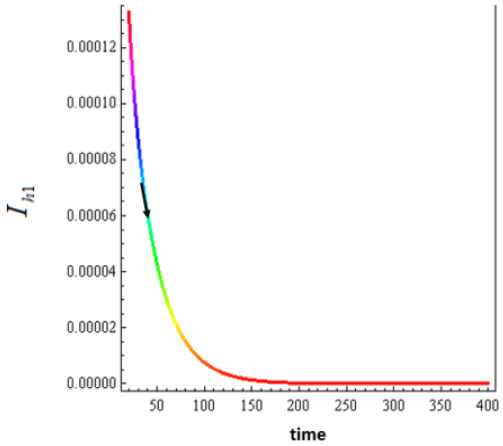

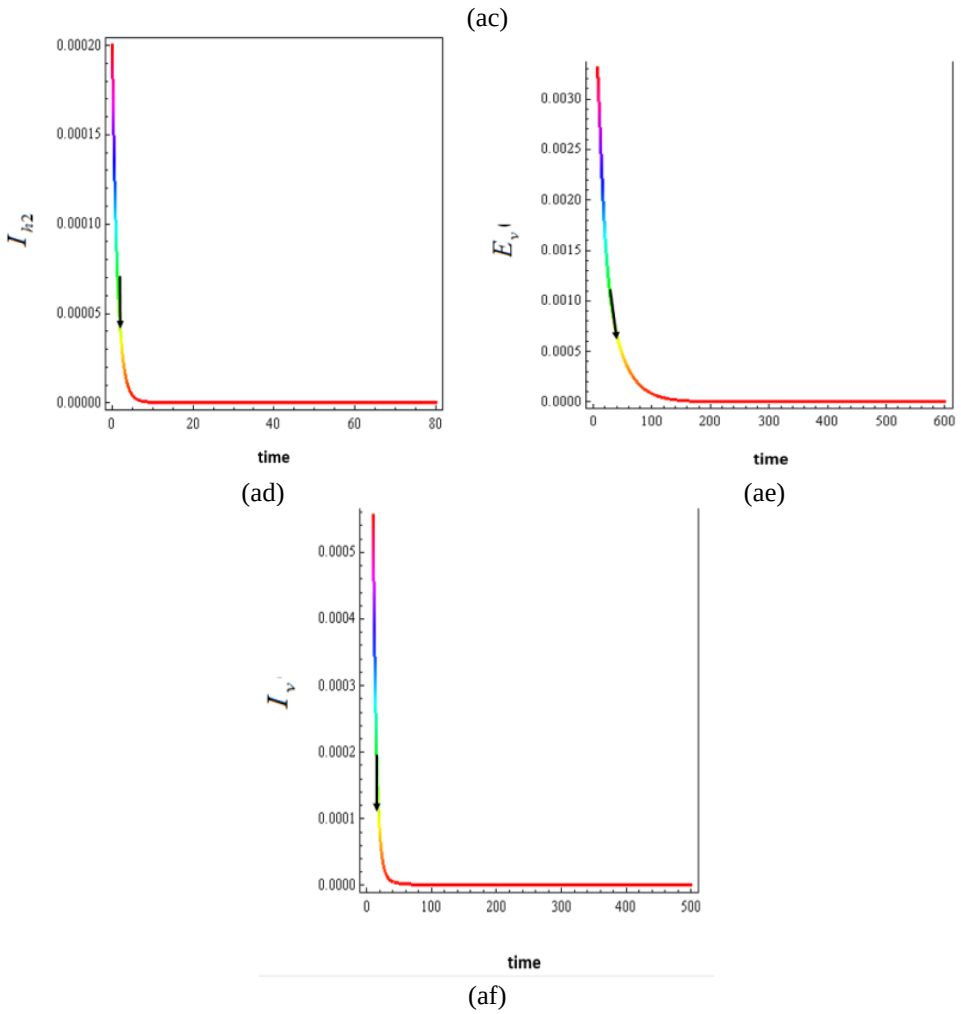

Figure 5. The time series of each population group

(aa) The time rate of change for the susceptible human population,
(ab) The time rate of change for the exposed population (infected but not yet transmit the dengue virus) at time,
(ac) The time rate of change for the DF patients,
(ad) The time rate of change for the DHF patients,
(af) The time rate of change for the exposed mosquitoes (infected but not yet transmit the dengue virus) at time,
(ae) The time rate of change for the infectious mosquitoes

The disease-free equilibrium is locally stable in support of the choice of parameter values within Table 2. The parameters used to generate the plots of Figure 5 are $\gamma_1 = 0.178$,

$\delta_{hh} = 1/(365*74)$, $\gamma_{hh} = 0.005$, $\gamma_{vv} = 0.009$, $\gamma_2 = 0.8$, $EP = 0.87$, $\alpha = 0.04$, $IP = 0.09$, $N_T = 100,000$, $N_{vv} = 3{,}000$, respectively.

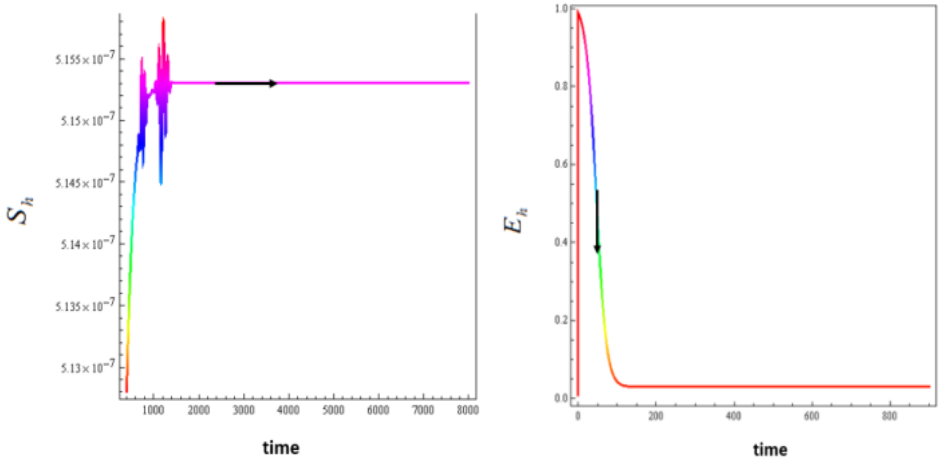

(a) (b)

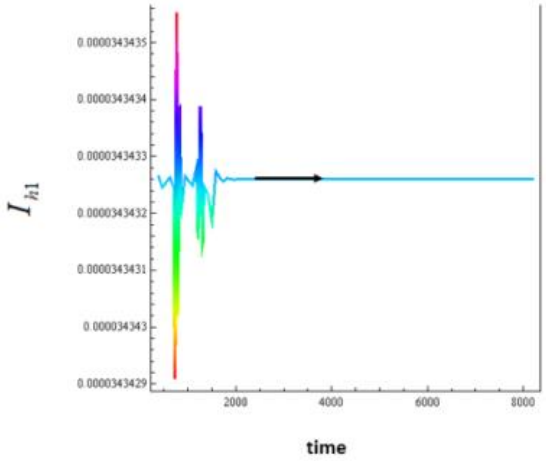

(c)

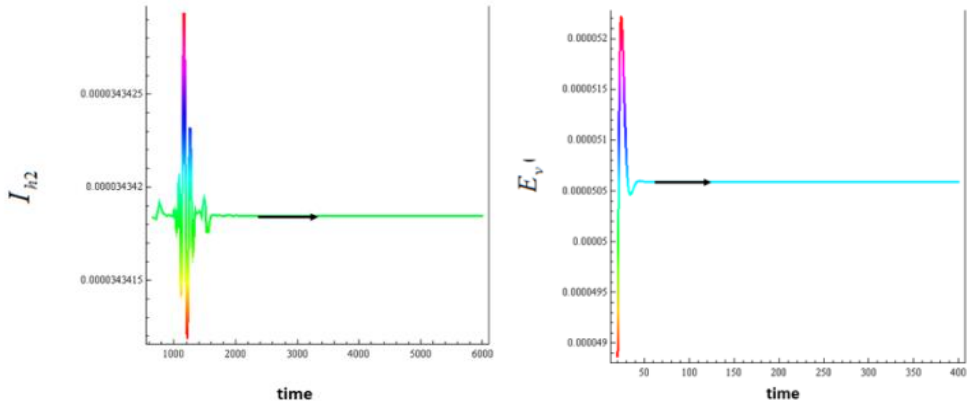

(e) (f)

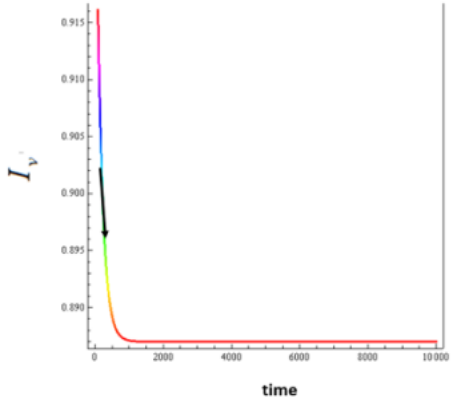

(g)

Figure 6. The time series of each population group

(a) The time rate of change for the susceptible human population,
(b) The time rate of change for the exposed population (infected but not yet transmit the dengue virus) at time,
(c) The time rate of change for the DF patients,
(d) The time rate of change for the DHF patients,
(f) The time rate of change for the exposed mosquitoes (infected but not yet transmit the dengue virus) at time,
(g) The time rate of change for the infectious mosquitoes.

The endemic equilibrium is locally stable within support of the choice for parameter values within Table 2. The parameters used to generate the plots of Figure 6 are $\gamma_1 = 0.178$, $\delta_{hh} = 1/(365*74)$, $\gamma_{hh} = 0.009$, $\gamma_w = 0.0008$, $\gamma_2 = 0.9$, $EP = 0.87$, $\alpha = 0.9$, $IP = 0.0006$, $N_T = 100{,}000$, $N_w = 3{,}000$, respectively.

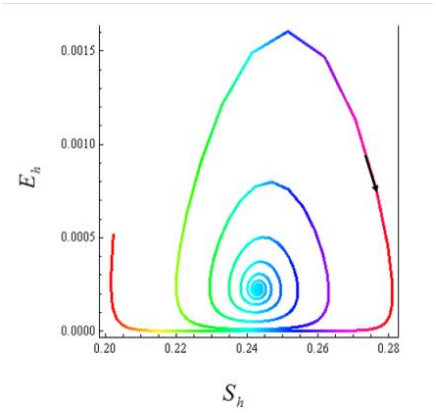
0.0015
0.0010
0.0005
0.0000
E_h
0.20
0.22
0.24
0.26
0.28
S_h

(aa)

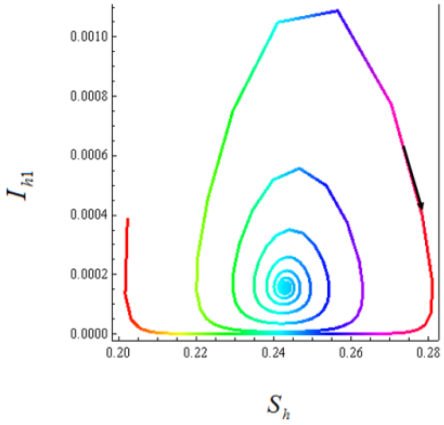
0.0010
0.0008
0.0006
0.0004
0.0002
0.0000
I_{h1}
0.20
0.22
0.24
0.26
0.28
S_h

(ab)

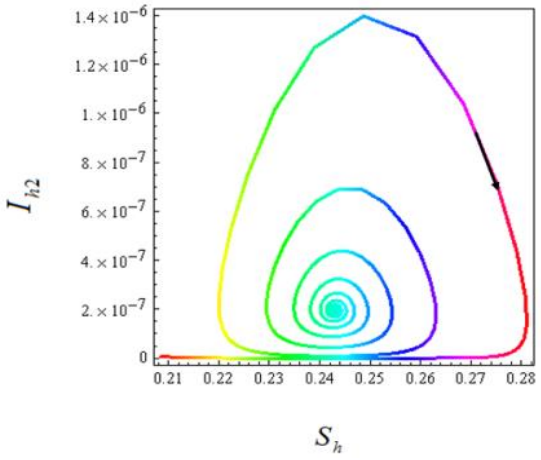
1.4×10^{-6}
1.2×10^{-6}
$1.\times10^{-6}$
$8.\times10^{-7}$
$6.\times10^{-7}$
$4.\times10^{-7}$
$2.\times10^{-7}$
0
I_{h2}
0.21
0.22
0.23
0.24
0.25
0.26
0.27
0.28
S_h

(ac)

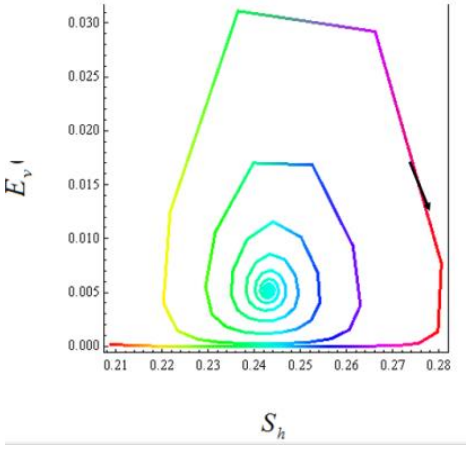
0.030
0.025
0.020
0.015
0.010
0.005
0.000
E_v
0.21
0.22
0.23
0.24
0.25
0.26
0.27
0.28
S_h

(ad)

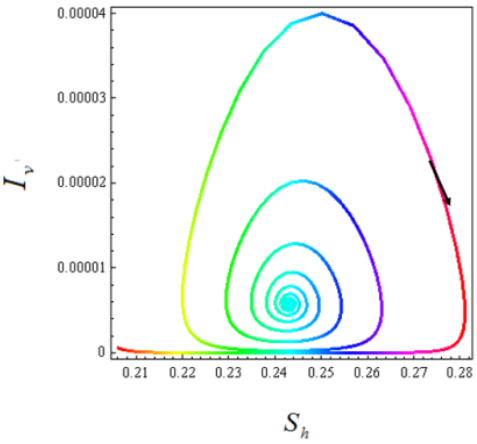
0.00004
0.00003
0.00002
0.00001
0
I_v
0.21
0.22
0.23
0.24
0.25
0.26
0.27
0.28
S_h

(ae)

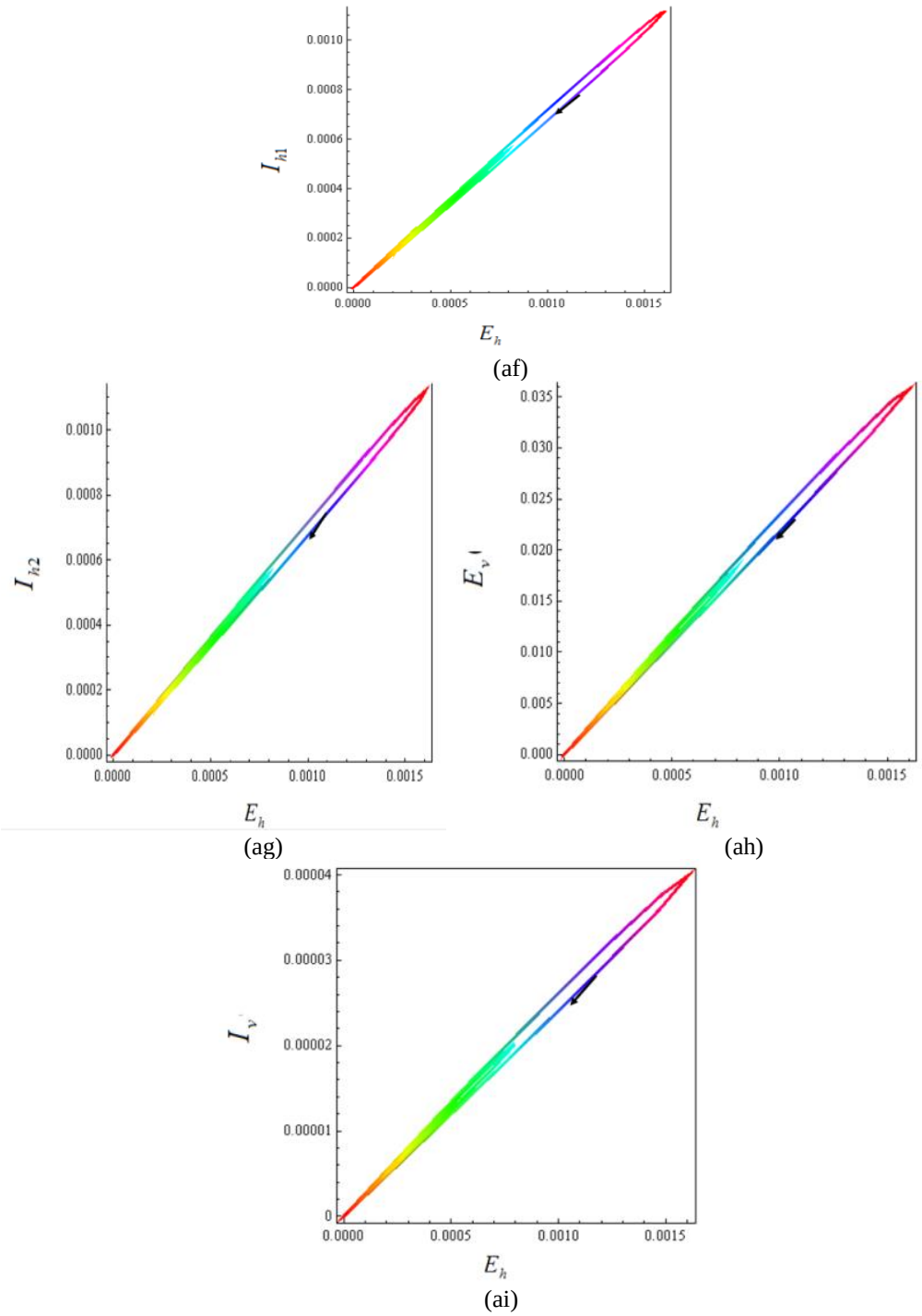

Figure 7. Numerical solution of (15)-(20) demonstrates the solution trajectory for each pair of population group

(aa) The solutions projected onto the coordinates (S_h, E_h)
(ab) The solutions projected onto the coordinates (S_h, I_{h1})
(ac) The solutions projected onto the coordinates (S_h, I_{h2})
(ad) The solutions projected onto the coordinates (S_h, E_v)
(ae) The solutions projected onto the coordinates (S_h, I_v)
(af) The solutions projected onto the coordinates (E_h, I_{h1})
(ag) The solutions projected onto the coordinates (E_h, I_{h2})
(ah) The solutions projected onto the coordinates (E_h, E_v)
(ai) The solutions projected onto the coordinates (E_h , I_v)

The endemic equilibrium is locally stable in support of the choice for parameter values within Table 2. The parameters used to generate the plots of Figure 7 are $\gamma_1 = 0.178$, $\delta_{hh} = 1/(365*74)$, $\gamma_{hh} = 0.009$, $\gamma_{vv} = 0.0008$, $\gamma_2 = 0.9$, $EP = 0.87$, $\alpha = 0.9$, $IP = 0.0006$ $N_T = 100{,}000$, $N_v = 3{,}000$, respectively.

4. Conclusions

In this paper, we analyzed the SEIR model for human populations and SEI model for mosquito population. The model is considered by taking into account infection times (primary and secondary infections). The results are to predict the developing tendency of disease and recovery. The model equations were solved analytically. We obtained the basic reproductive number R_0, when $R_0 < 1$. The trajectory approaches the disease-free equilibrium point such as indicated within Figure 5. The trajectory solutions approached to the endemic equilibrium point as shown in Figure 6. The R_0 is given as follows:

$$R_0 = \frac{N_T N_{vv} (\delta_{hh} + \alpha + \gamma_2) \gamma_{hh} \gamma_{vv} \mu_{hh}}{\delta_{hh}(1+\delta_{hh} IP)(\delta_{hh} + \alpha + \gamma_1)(\delta_{hh} + \gamma_2)\mu_{vv}(1+EP\mu_{vv})} \tag{32}$$

Based on the epidemiological data, we estimated R_0 for the dengue sequential infection in Thailand. The implication of this point is to feasible defect for the model.

Next, we compare the behavior solutions of each population group between SEIR and SIR model for human population. The basic SIR model is derived simply by removing the exposed human population compartment E_h. Specifically, Equations (1)-(5) are now rewritten as follows:

$$\frac{dS_h}{dt} = \mu_{hh} N_T - \gamma_{hh} S_h I_{vv} - \delta_{hh} S_h \tag{33}$$

$$\frac{dI_{h1}}{dt} = \gamma_{hh} S_h I_v - \delta_{hh} I_{h1} - \gamma_1 I_{h1} - \alpha I_{h1} \tag{34}$$

$$\frac{dI_{h2}}{dt} = \alpha I_{h1} - \delta_{hh} I_{h2} - \gamma_2 I_{h2} \tag{35}$$

$$\frac{dR_h}{dt} = \gamma_1 I_{h1} + \gamma_2 I_{h2} - \delta_{hh} R_h \tag{36}$$

The parameters used to compute the behavior solutions of Equations (33)-(36) are kept the same as the SEIR model. Figure 8 (i) plots the responses of the SEIR model, while Figure 8 (ii) plots the responses of the SIR model of Equations (33)-(36). We can see that the solutions of SEIR model converge to the equilibrium states faster than SIR model. The parameters of SIR model are the same as in SEIR model.

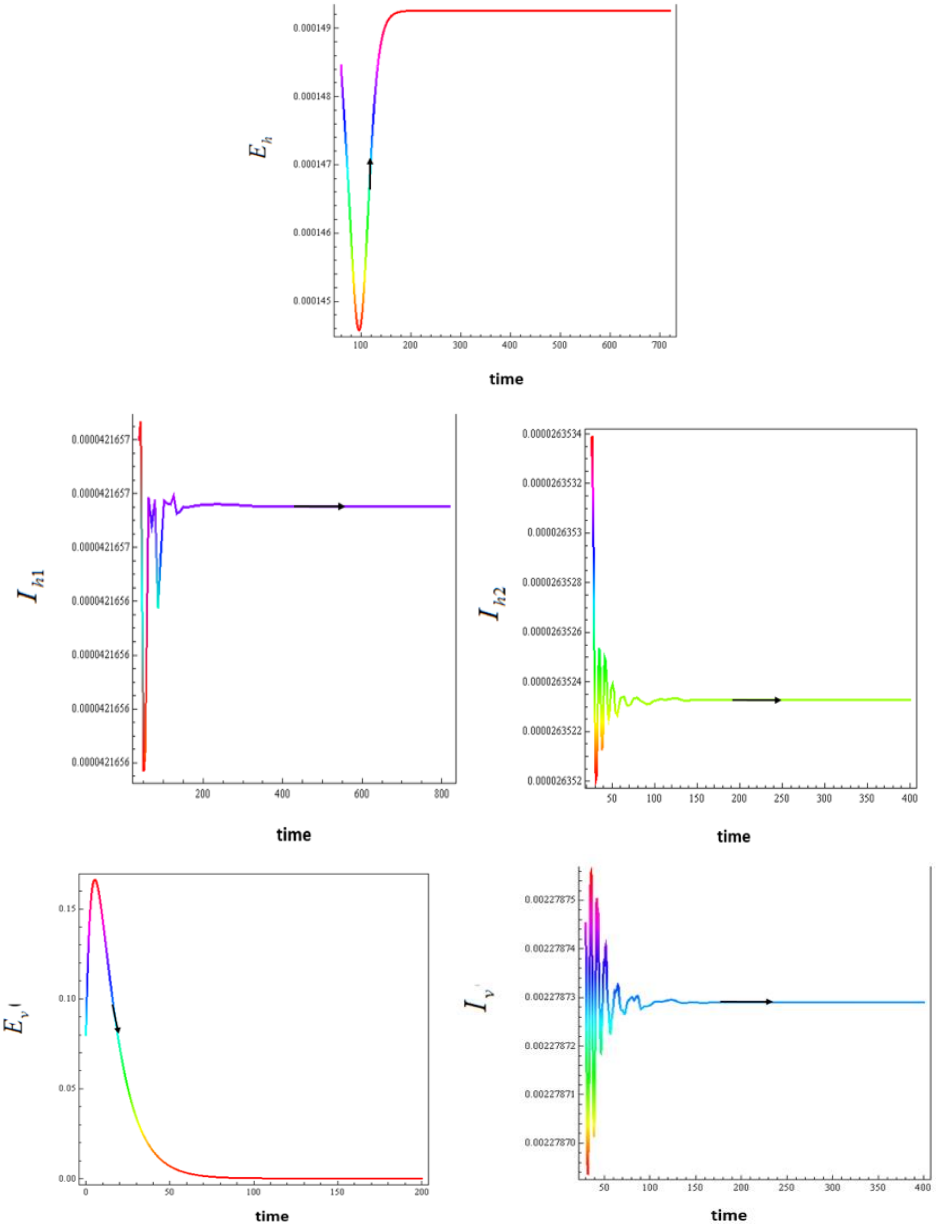

(i) Behavior in structured SEIR model

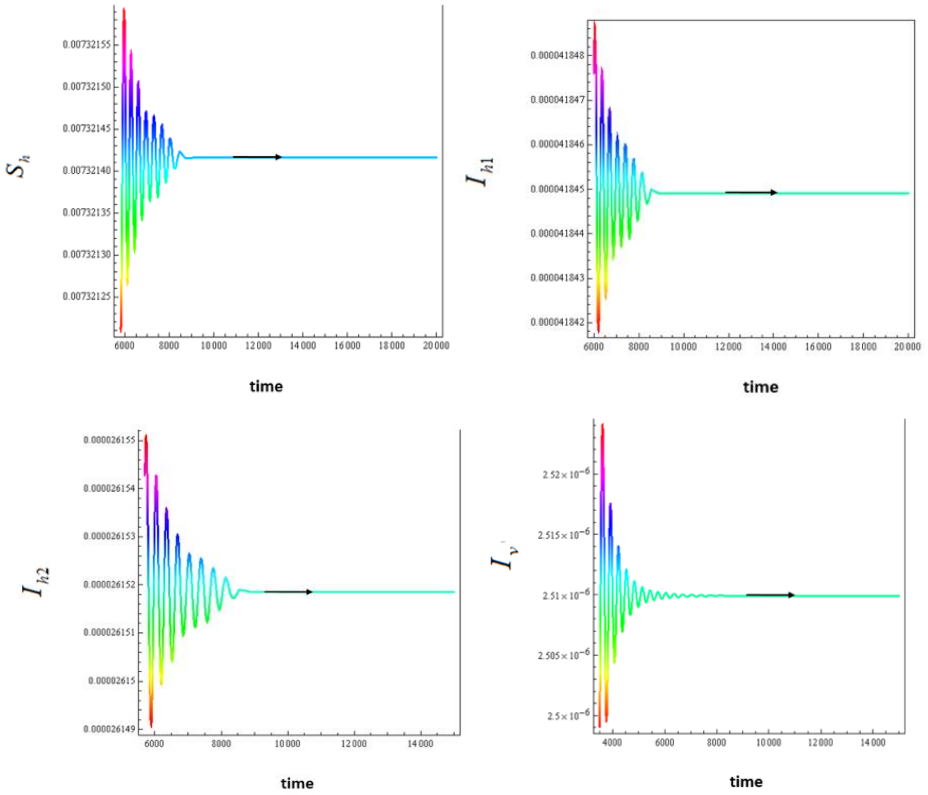

(ii) Behavior in structured SIR model

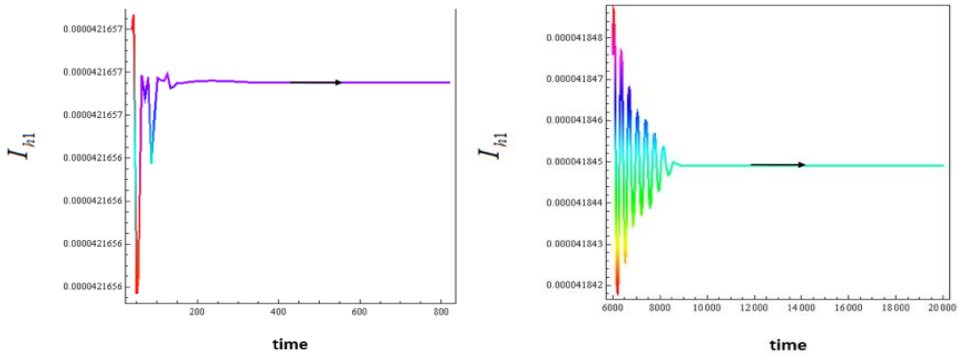

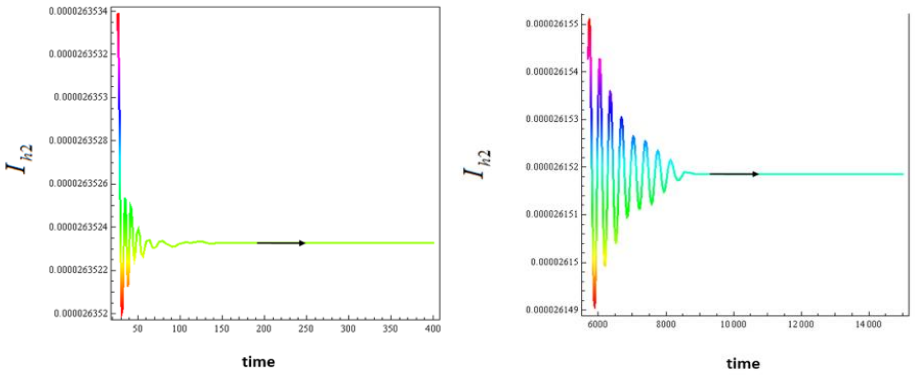

(iii) Behavior in I_{h1} and I_{h2} structured SEIR model (iv) Behavior in I_{h1} and I_{h2} structured SIR model

Figure 8. Plot of number of susceptible and infected humans in SEIR model and SIR model

(i) The time series for each of population group for the SEIR model. The parameters are $\gamma_1 = 0.178$, $\delta_{hh} = 1/(365*74)$, $\gamma_{hh} = 0.007$, $\gamma_{vv} = 0.0003$, $\gamma_2 = 0.8$, $\alpha = 0.5$, $N_T = 100,000$, $N_{vv} = 5,000$, $EP = 0.09$, $IP = 0.0008$ and $R_0 = 15.47$. The solutions converge in support of the endemic disease state (0.0000455,0.15546, 0.0000979, 0.000002448, 0.36766, 0.004406). It is seen that the solutions oscillate to the endemic disease state.

(ii) The time series of each population group for the SIR model. The parameters are $\gamma_1 = 0.178$, $\delta_{hh} = 1/(365*74)$, $\gamma_{hh} = 0.007$, $\gamma_{vv} = 0.0003$, $\gamma_2 = 0.8$, $\alpha = 0.5$, $N_T = 100,000$, $N_{vv} = 5,000$ and $R_0 = 19.17$. This model has no E_{hh} and E_{vv} . The solutions approach to the endemic disease state (145.95425, 0.0299943, 0.00003742, 0.001838). We can see that the responses oscillate to the endemic disease state.

For the simulation seen in Figure 8 (iii) for SEIR model and (iv) for SIR model the existing only in the imagination part of the complex roots is roughly 0.002698 and 0.014759. Thus, we can forecast the period with the oscillations as they approach P_1 by method of the solutions of the linearized system, acquiring $2\pi/0.002698 \approx 6.38$ years and $2\pi/0.014759 \approx 1.17$ years, respectively.

5. Acknowledgements

The authors would like to thank Research and Development Institute, Faculty of Science and Technology, Phuket Rajabhat University and Faculty of Science, King Mongkut's Institute of Technology Ladkrabang.

References

[1] Bureau of Epidemiology, 2017. Department of Disease Control, Ministry of Public Health, Thailand. [online] Available at: http://www.boe.moph.go.th/fact/ Dengue_ Haemorrhagic_ Fever.htm

[2] Hanson, J.L. and Fischer, P.R., 2017. Ready for Dengue in the United States? [online] Available at: https:// www.ahcmedia. com /articles/140960-ready-for-dengue-in-the-united-states

[3] Wikipedia, 2017. Dengue Virus. [online] Available at: https://en.wikipedia.org/wiki/ Dengue_virus.

[4] Structure of Dengue Virus, 2017. BioInteractive. [online] Available at: https://www.hhmi.org/biointeractive/structure-dengue-virus.

[5] Immunization, Vaccines and Biologicals, Word Health Organization, 2017. [online] Available at: https://www.who.int/immunization/research/development/dengue_vaccines/en/.

[6] Kongnuy, R. and Pongsumpun, P., 2010. Mathematical Modeling for Dengue Transmission with the Effect of Season. *International Journal of Biological and Medical Sciences*, 5(2), 74 -78.

[7] Esteva, L. and Vargas, C., 1998. Analysis of a dengue disease transmission model. *Mathematical Bioscience*, 150, 131-151.

[8] Sungchasit, R. and Pongsumpun, P., 2012. Dengue transmission model with the different incubation rate for each season. *1st Mae FahLuang University International Conference 2012*, Chiangrai, 1-12.

[9] Nikin, B.R. and Ciupe, S.M., 2017. Modelling original antigenic sin in dengue viral infection. *Mathematical Medicine and Biology*, 35(2), 1-16.

[10] Pongsumpun, P. and Tang, I.M., 2003. A realistic age structured transmission model for dengue hemorrhagic fever in Thailand. *Mathematical and Computer Modelling 32*, 336-340.

[11] Thavara, U., Tawastsin, A., Chansang C., Kong-ngamsuk, W., Paosriwong, S., Boon-Long, J., Rongsriyam, Y., Komalamisra, N., 2001. Larval occurrence, oviposition behavior and biting activity of potential mosquito vectors of dengue on Samui Island, Thailand. *Journal of Vector Ecology*, 26(2), 172-180.

[12] World Health Organization, 2009. *Dengue: Guidelines for Diagnosis, Treatment. Prevention and Control*. Geneva: World Health Organization and the Special Programme for Research and Training in Tropical Diseases.

[13] Guidance Clinical, 2017. Centers for Disease Control and Prevention. [online] Available at: https://www.cdc.gov/dengue/clinicallab/clinical.html.

[14] Syafruddin, S. and Noorani, M., 2012. SEIR model for transmission of dengue fever in Selangor Malaysia. *International Journal of Modern Physic: Conference Series*, 9, 380- 389.

[15] Kerdpanich, A., Watanaveeradej, V., Samakoses, R., Chumnanvanakij, S., Chulyamitporn, T., Sumeksri, P., Vuthiwong, C., Kounruang, C., Nisalak, A. and Endy, T., 2001. Perinatal dengue infection, *Southeast Asian Journal of Tropical Medicine and Public Health*, 32(3), 488-493.

[16] Ferguson, N., Donnelly, C. and Anderson, R., 1999. Transmission dynamics and epidemiology of dengue: insights from age-stratified sero-prevalence surveys. *Philosophical Transactions of the Royal Society London B. Biological Science*, 354, 757-768.

[17] Changal, K., Raina, A.B., Raina, A., Raina, M., Bashir, R., Latief, M., Mir, T. and Changal, Q., 2016. Differentiating secondary from primary dengue using IgG to IgM ratio in early dengue: an observational hospital based clinico-serological study from North India. *BMC Infectious Diseases*,16(1),715-721.

[18] Guzman, M.G., Mayling, A. and Halstead, S.B., 2013. Secondary infection as a risk factor for dengue hemorrhagic fever/dengue shock syndrome: an historical perspective and role of antibody-dependent enhancement of infection. *Archives of Virology*, 158(7), 1445-1459.
[19] Diekmann, D. and Heesterbeek, J., 2000. *Mathematical Epidemiology of Infectious Disease: Model Building, Analysis and Interpretation*. Chichester: John Wiley and Sons Ltd.
[20] Adams, B., Holmes, E.C., Zhang, C., Mammen, M.P., Nimmannitya, S., Kalayanarooj S. and Boots, M., 2006. Cross-protective immunity can account for the alternating epidemic pattern of dengue virus serotypes circulating in Bangkok. *Proceedings of the National Academy of Sciences*, 103(38), 14234-14239.
[21] Annual Epidemiological Surveillance Report, 1992-2012. Division of Epidemiology, Ministry of Public Health, Royal Thai Government.
[22] Sungchasit, R., Pongsumpun, P. and Tang, I.M., 2015. SIR transmission model of dengue virus taking into account two species of mosquitoes and an age structure in the human population. *American Journal of Applied Sciences*, 12(6), 426-443.
[23] Cheah, W.K., Ng, K.S., Marzilawati, A.-R. and Lum, L.C.S., 2014. A review of dengue research in Malaysia. *Medical Journal of Malaysia*, 69 (Supplement A), 59-67.
[24] Pongsumpun, P. and Tang, I.M., 2003. Transmission of dengue hemorrhagic fever in an age structured population. *Mathematical and Computer Modelling*, 37, 949-961.
[25] Omic, J. and Van Mieghe, P., 2016. Epidemic spreading in networks-variance of the number of infected nodes. [online] Available at: https://www.nas.ewi.tudelft.nl/people/Piet/papers/VirusSpread_VarianceTUDReport20090707.pdf